13th ewtec 2019 Proceedings of the 13th European Wave and Tidal Energy Conference 1-6 Sept 2019, Naples, Italy

Numerical modelling of the impact of hydrokinetic turbine on the morphology of the near sandy bed

Fatima Khaled, Sylvain Guillou, Yann Méar and Ferhat Hadri

Abstract— **Interactions between hydrokinetic turbines and the near scale and far scale bed sediments are considered as a critical area of assessment, however limited research studies have been published to address this issue. The aim of the present contribution is to model the impact of the presence of horizontal-axis turbine with the flow and a mobile sediment bed. A modelling framework is derived to predict the scour induced by the turbine installed on fluvial erodible sandy bed surfaces, such as the Eulerian multiphase model for sediments and Blade Element Momentum Theory (BEMT) for turbine, using the open source plateform OpenFOAM. It has been shown that the scouring capabilities are well enhanced below the turbine due to the acceleration of the flow and increasing of local shear stress of sediments.**

Keywords—**Environmental Impact, Euler-Euler multiphase, Hydrokinetic Turbines, Numerical Simulations, OpenFOAM.**

I. Introduction

THE need of sustainable, predictable energy has led in recent years to the development of projects and studies concerning the installation of Hydrokinetic Turbines (HT) in such high currents regions as Alderney Race, Race of Barfleur, The Rhône … [1].

Accelerating marine hydrokinetic renewable energy development towards endurance requires investigating interactions between the manufactured environment and its surrounding physical environment.

The ID of this paper is: 1683, the conference track is Environmental Impact and Appraisal, (EIA).
"The authors acknowledge CRIANN (Centre Régional Informatique et d'Application Numériques de Normandie) co-financed by the Normandy Region, the State and the European Union, for the access to the Computation means and to the Manche Country Concil for their founding"

F.Khaled and S.Guillou are at University of Normandy, UNICAEN LUSAC, EA 4253, 60 rue Max Pol Fouchet, CS 20082, 50130 Cherbourg, France. (e-mail : fatima.khaled@unicaen.fr ; sylvain.guillou@unicaen.fr)
Y.Méar is in INTECHMER/LUSAC, Bd de Collignon, 50110 Tourlaville, France. (e-mail: yann.mear@lecnam.net)
F.Hadri is in LISV, University of Versailles, 78140 Vélizy, France. (ferhat.hadri@uvsq.fr).

Regional modelling with a representation of the turbines' array with bed friction or momentum sink approach were proposed to quantify the impacts far away from the turbines.

Sanchez and al. [2] have applied a 3D numerical model in Ria de Ortigueira to study the potential flow changes due to the operation of a steam turbines' farm. It was found that the resulting transient flow modifications were concentrated in the area occupied by and next to the farm, with nearly negligible effects outside the inner Ria. Fairley et al. [3] studied the cumulative impact of HT on sediment transport in the Pentland Firth and have concluded that the array implementation only has minimal effect on the baseline morphodynamics of the large sandbanks in the region. Neill et al. (2009, 2012) used large grid-cell simulations to estimate the impact of an HT array on the sand banks off the northern coast of France. The study investigated a tidal channel many kilometers long, therefore lacking there solution to simulate the near-field effects.

To date, few studies exist on how HK devices modify erodible channels nearby distance downstream of the turbine, despite it is important to develop a holistic understanding as to how these devices affect all aspects of physical environments. Hill et al. [4] have shown experimentally that the presence of the turbine and the rotation of the blades impact the bed morphology. Therefore, the interaction between HT and the bed morphology deserves more studies.

The present contribution investigates the impact of the deployment of riverine turbines on the evolution of the sandy bed close to the turbine by CFD modelling framework.

The methodology, provided in section II, is based on the two-phase flow Euler-Euler 3D CFD model to simulate the sediment transport and the morphology evolution around the turbine (Chauchat and Guillou [5] , Bonamy et al.[6], Zhen Cheng et al. [7]) and the hybrid analytical 3D Blade Element Momentum Theory (BEMT) is used to compute the effect of energy extracted from the turbine on the fluid in the near wake (Malki et al.[8], Shives et al.[9]). The CFD open source library OpenFoam has been used, the SedFoam code [6] which is based on twoPhaseEulerFoam code, is applied with introducing the momentum source code of the turbine.

Then section III addresses the interactions between an axial-flow turbine and a sand bedload transport. At the end, section VI discusses the results and presents several conclusions.

II. Numerical Methods and Validation

A. Hydrokinetic turbine modelling

The momentum theory is often applied to predict the power output, the thrust and the efficiency of a hydrokinetic turbine. The model is an hybrid analytical, BEM, and CFD computational model.

1) BEMT

The blade element theory is considered as a more advanced analysis of the hydrodynamic behavior of hydrokinetic turbine in addition to the analysis of energy extraction process examined by the actuator disk model. It allows considering the effects of rotor geometry characteristics like chord and twist distributions of the blade airfoil. The blade is separated into radial sections since each of the blade elements has a different rotational speed and geometric characteristics hence experiencing a slightly different flow (Figure 1). Moreover, the forces and moments are determined in each element so that total forces and moments are calculated by integrating the individual forces and moments on each element. In the present study, the Blade Element Momentum (BEM) theory is adopted as the main computation method and it is applied over a disc that represents the turbine with radius r, thickness e and number of blades n.

The turbine hydrodynamics efforts are represented as a momentum source term S_i in equation (6). The lift force acts perpendicular to the relative velocity, while the drag acts parallel:

$$L = \frac{1}{2}\rho c V_{rel}^2 C_L F_{tip}$$
$$D = \frac{1}{2}\rho c V_{rel}^2 C_D \quad (1)$$

where c is the chord of the blade which varies in function of radius, C_L and C_D are lift and drag coefficient respectively, their values depend on the geometry of the blade (angle of attack), V_{rel} is the relative velocity of the water flow such as:

$$V_{rel} = \sqrt{V_{axial}^2 + (r\omega - V_\theta)^2} \quad (2)$$

The lift and drag forces are rotated into the rotor's cylindrical coordinate system to obtain axial and tangential force components:

$$f_x = L\cos\emptyset + D\sin\emptyset$$
$$f_\theta = -D\cos\emptyset + L\sin\emptyset \quad (3)$$

The momentum sources are computed based on the time-averaged blade forces (per unit cell volume) imparted by the blade onto the fluid as it traverses through the water. The source term S_i is projected with reference to cylindrical coordinate system, S_x and S_θ, such as:

$$S_x = \frac{nf_x}{2\pi re}$$
$$S_\theta = \frac{nf_\theta}{2\pi re} \quad (4)$$

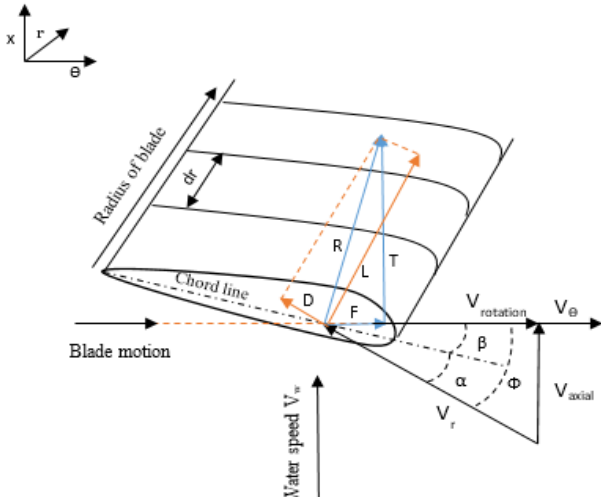

Fig. 1. Flow velocities and forces acting on the blade by BEMT. Vaxial, VΘ are the axial and tangential velocity components, β is the blade twist angle, α the angle of attack, Ø the inflow angle.

The final sources Si in the Cartesian coordinate system are obtained by a projection of the cylindrical source terms. The total thrust T and power P is calculated by numerical integration of the sources over the disc region.

2) Validation

The experimental measurements of Mycek et al. [13] has been exploited. The experiments were performed in the IFREMER's experimental flume tank, which has a length of L=18m, a width of l = 4m and a depth of h=2m. Figure 2 shows the tidal turbine used in the experiments. The rotor of diameter d = 0.7m is connected to a 0.72 m long cylindrical hub of diameter 0.092 m. The chosen case has the following characteristics showed in table 1.

The geometry and mesh are created using ICEM CFD software. Structured hexahedral cells were used to mesh the entire domain, which comprises of approximately 1.3 million cells. The rotor domain mesh was of structured hexahedral mesh used for CFD-BEMT with diameter d=0.7m. The computational domain is a 4m x 18m x 2m block. The disc is located at 11D downstream the inlet

boundary to avoid interactions with this inlet. This lets 14D downstream to observe the development of the wake.

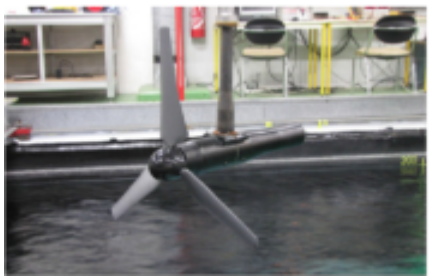

Fig. 2. Picture of the tidal turbine used during the experiments of Mycek et al. (2014).

Table 1: Description of parameters used in Mycek [13] experiment; U∞: flow velocity, TSR: Tip Speed Ratio (ωd/2U∞), I: Turbulence Intensity.

Profile	U∞	TSR	Re	I	Pitch	Rotation
NACA 63418	0.8 m/s	3.67	28^{e4}	3%	0^{o}	counter-clockwise

As in the experimental case, an ambient turbulence intensity rate I∞=3% is adopted. The mesh of areas in interest is refined to concentrate accuracy. The hub is represented as a solid cylinder in the centre of the disc with radius 0.046m. The blades are modelled using 23 discrete NACA 63418 elements along their span in accordance with the detailed blade profile description given in [13]. The averaged value of the incident flow velocity 0.8 m.s^{-1} is considered.

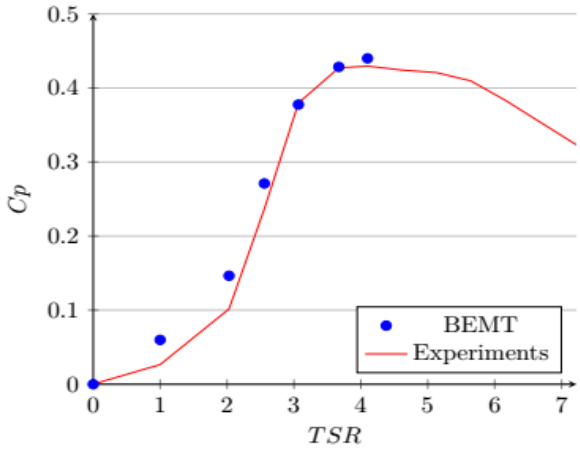

Fig. 3. Variation of Power coefficient in function of TSR factor.

According to figure 3, a good agreement is observed on the Cp evolution for TSR values from zero to 3.67. A better agreement is obtained as the TSR increases until 3.67. This could be explained regarding the tidal turbine geometry (no mast modelling) so the vortices generated on the tip of blades and on the hub are taken into account. Since we consider from the beginning a simple correction on the tip, while in literature there exist other corrections for BEMT that might be considered. For TSR=3.67, the absolute errors according to experiment measurements are 0.3% for CP.

B. Sediment Transport

1) Multiphase Euler Model

The mathematical formulations of the Eulerian two-phase flow model is obtained by averaging the local and instantaneous mass and momentum conservation equations for fluid and particles phases [5, 6, 7, 10, and 11]. In the present model, the turbulence time averaged Eulerian two-phase flow equations described in Chauchat et al. [5] and implemented in the open source finite volume CFD library [6].

The mass conservation equations for the particle phase and fluid phase are written as:

$$\frac{\partial \phi}{\partial t} + \frac{\partial \phi u_i^s}{\partial x_i} = 0$$
$$\frac{\partial (1-\phi)}{\partial t} + \frac{\partial (1-\phi) u_i^f}{\partial x_i} = 0 \quad (5)$$

where ϕ , and 1-ϕ are the particle and fluid volume fractions, u_i^s, u_i^f are the sediment and fluid phase velocities, and the index i=1, 2, 3 represents the streamwise, spanwise and vertical component, respectively. The momentum equations are written for each phase. The index k designs the phase ('f 'for the fluid phase, 's' for the solid phase)

$$\frac{\partial \rho^s \phi u_i^s}{\partial t} + \frac{\partial \rho^s \phi u_j^s u_i^s}{\partial x_j} = -\phi \frac{\partial p}{\partial x_i} + \phi f_i - \frac{\partial p^s}{\partial x_i} + \frac{\partial \tau_{ij}^s}{\partial x} + \phi \rho^s g_i + \phi(1-\phi)K\left(u_i^f - u_i^s\right) - \frac{1}{S_c}(1-\phi)K v_t^f \frac{\partial \phi}{\partial x_i} + S_i \quad (6)$$

Where ρ^s, ρ^f are the particle and the fluid density, g_i is the gravitational acceleration and p is the fluid pressure. τ_{ij}^f is the fluid stress (viscous stress and fluid Reynolds stresses), p^s is the normal stress of particles and τ_{ij}^s their shear stress. The terms K and S_c are the drag parameter and Schmidt number respectively of particles. S_i is the Reynolds Averaged momentum source term it represents the turbine's forces imposed on the flow.

The turbulence model k-ε described by Cheng et al. [7] from Hsu et al. [11] has been used.

2) Validation

The model is implemented numerically and it is validated by an experience realized in LMSGC (Pham Van Bang et al. [12]) consisting of suspension of polystyrene beads (d = 290 μm, ϱs = 1050 kg/m3) of volume fraction 0.48, in silicone oil (ϱf = 950 kg/m3). The numerical results

and experimental measurements of sedimentation process during the time are reported. Comparing results on the temporal evolution of the vertical position of the interfaces and the concentration profiles allows showing the capacity of the approach to represent the process of sedimentation.

III. INTERACTIONS BETWEEN BEDLOAD AND TURBINE

An attempt has been made to simulate the effect of stream turbine on the transport of contouring sediments; a first approach consists on considering a unique type of sediments, the sands, and a unique axial flow direction, corresponding to the riverine turbine case.

A. Application Setup

1) Numerical properties

The mesh is created using OpenFOAM package, it is configured as 20 million hexahedral mesh, which captures a rectangular domain with, dimensions 2m x 0.35m x 0.4m, in x, y and z directions. The mesh is refined on the bottom of the domain where a sand sheet of thickness equal to 0.05m, and volume fraction of 0.61, is spread out (see figure 4).

The initial and inlet conditions for velocity are set to a logarithmic profile. Neumann boundary condition is applied to the bottom whereas hydrostatic pressure is fixed at outlet. The turbulent kinetic energy is set such as the turbulence intensity is 3% at the inlet.

The angular velocity of the turbine used in the present work is calculated basing on TSR=3, the blades are modelled using 23 discrete NACA 63418 elements along their span in accordance with the detailed blade profile description given in [13].

2) Transport properties

The model is calibrated with medium-diameter of sands ($d = 0.25$ mm, $\rho^s = 2100$ kg.m^{-3}) in the sheet flow condition. Concerning the closure models for granular constraints, either for the shear induced or for collisional stresses, the kinetic theory is applied. The model for particles viscosity and conductivity is the one of Syamlal [11], and the theories of Lun [11] is used for the granular pressure. The limit volume fraction is set to 0.635, to prevent unphysical sediment concentration in the bed. The drag model used for both faces is Gidaspow Schiller Naumann [11].

The turbulent suspension of particles is taken into consideration, since the unsteady turbulent URANS model is used. For that purpose, a very small time step is imposed to approach to the convergence.

In the present contribution, the results are mostly analysed at three sections: the first one is below the turbine at x/d=5.25, the second is downstream the turbine at x/d=6.75 and the last is at a further distance x/d=8.125, as shown in figure 4.

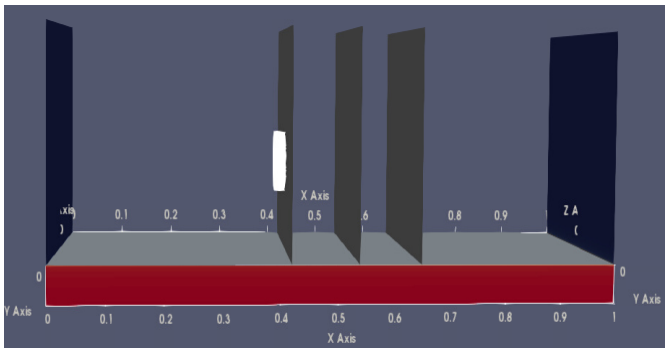

Fig. 4. Initial state of domain, position of the disc (white color) and three consecutive sections downstream: at x/d=5.25, x/d=6.75 and x/d=8.125 respectively.

B. Results and discussions

In the present contribution, the results are mostly analysed at three sections: the first one is below the turbine at x/d=5.25, the second is downstream the turbine at x/d=6.75 and the last is at a further distance x/d=8.125, as shown in figure 4.

1) Temporal Evolution

Figure 5 shows the evolution of the morphology during the time on three sections: below the turbine at x/d=5.25 and downstream the turbine at x/d=6.75 and x/d=8.125. It is evident that the scour occurs in the first 13s below the turbine, the bed elevation decreases progressively; however, it dropped sharply and evolve constantly around 0.044d to reach an equilibrium state. This is due to the gap increased between the rotor tip and the sands surface, which leads to decrease the local acceleration and local shear stress initially responsible for erosion in the near field region.

Otherwise, at a further distance downstream the turbine, at x/d=6.75, the elevation of the bottom progresses downward but in the form of crests and hollows, it has the tendency to reach its equilibrium state at an instant, t=17s, greater than the one occurred below the turbine. This explains that the local sediments eroded by the turbine continues to be transported by the wake even after t=13s, that is why there is variation of bottom elevation between t=13s and t=17s at x/d=6.75.

However, the case at x/d=8.125 is extremely different. The erosion evolution is much slower than the previous cases. During the 20s; the curve of bed elevation evolution is not well decreasing, on the contrary, there is an evident crest formed at t=16s, referring to the diminution of the shear stress at this time: the sediments eroded from downstream the turbine are transported by the wake to be deposited at x/d=8.125. They come from the erosion that is taken up at x/d=6.75 from t=13s to 15s, then this crest is ripped out progressively due to the tip induced acceleration.

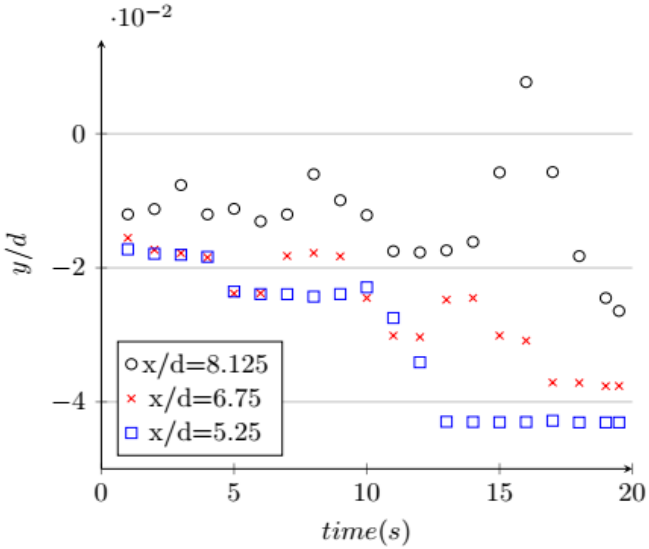

Fig. 5. Temporal evolution of the scour at three sections on the same line at x/d=5.25, x/d=6.75 and x/d=8.125.

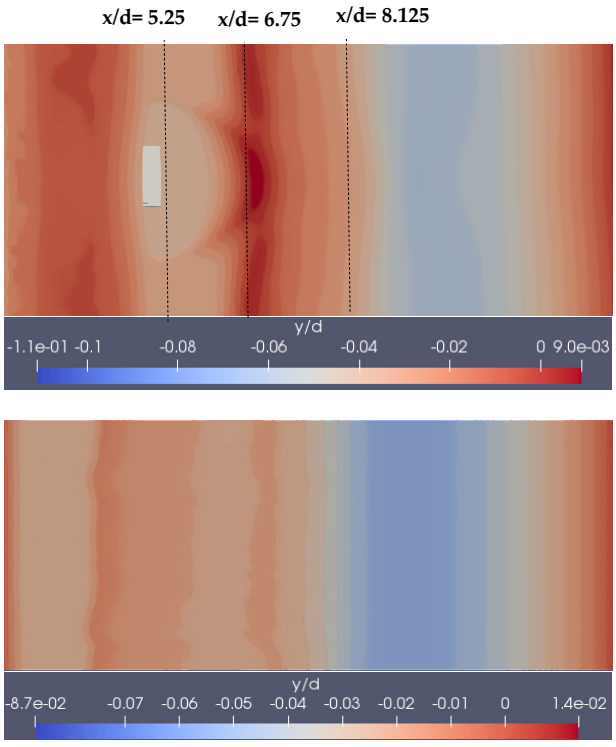

Fig. 6. Elevations of the bottom in presence of the turbine (up) and baseline case (down) at t=17s.

The equilibrium state occurred below the turbine at x/d=5.25 is taken into consideration in the next section, all the results presented afterwards are on the equilibrium interval time, especially on t=17s.

2) Spatial Evolution

Figure 6 shows the modifications of the sediment bed at the streamwise channel centreline throughout the simulation, with and without the rotor. Several changes in bed morphology have been found in the presence of the rotor. The clearest feature is the scour in the near wake area immediately after the rotor, about 0.025d more eroded sands in the area under the turbine comparing to the baseline results, due to two factors.

First, an increase in bed shear stress just below the turbine is occurred, which explains that the presence of turbine increases the local shear stress directly downstream of its location and greatly enhances scour below the turbine and deposition downstream.

Second, the local flow acceleration resulting from flow shrinking between the rotor bottom tip and the approaching dune crest (see figure 7). This acceleration decreases the crest elevation below the turbine, forms a scour and leads subsequently to a varied morphology downstream the turbine.

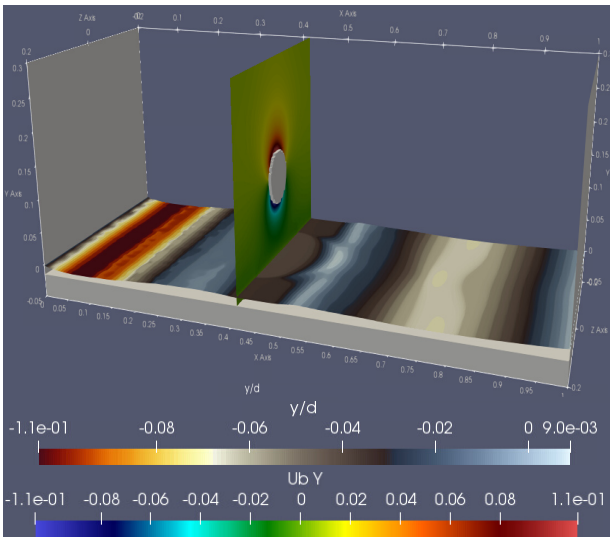

Fig. 7. Vertical wake representation causing the erosion below the turbine.

Figure 8 shows clearly the bed morphology changes that can occur in the downstream cross-stream sections due to the presence of the turbine. Just below the turbine at 5.25d, the double amount of sand is eroded comparing with the baseline results, about 0.04d the total elevation of the scour.

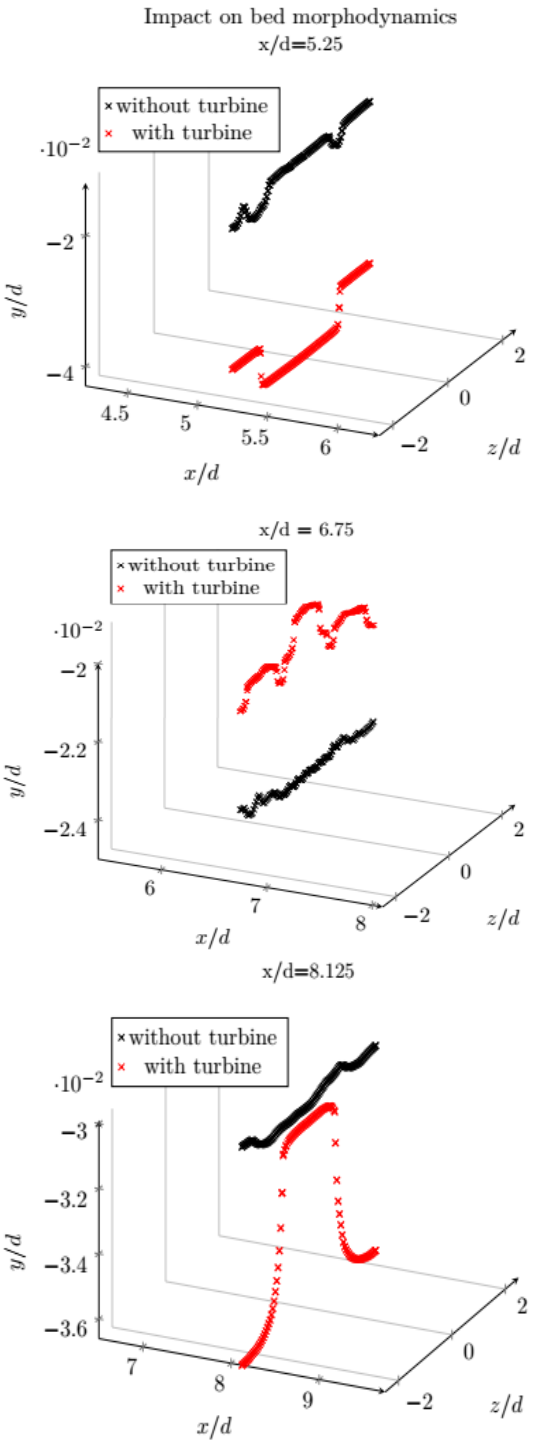

Fig. 8. Evolution of the dimensionless bed elevation at three cross-stream sections downstream the turbine: (a) x/d=5.25, (b) x/d=6.75 and (c) x/d=8.125.

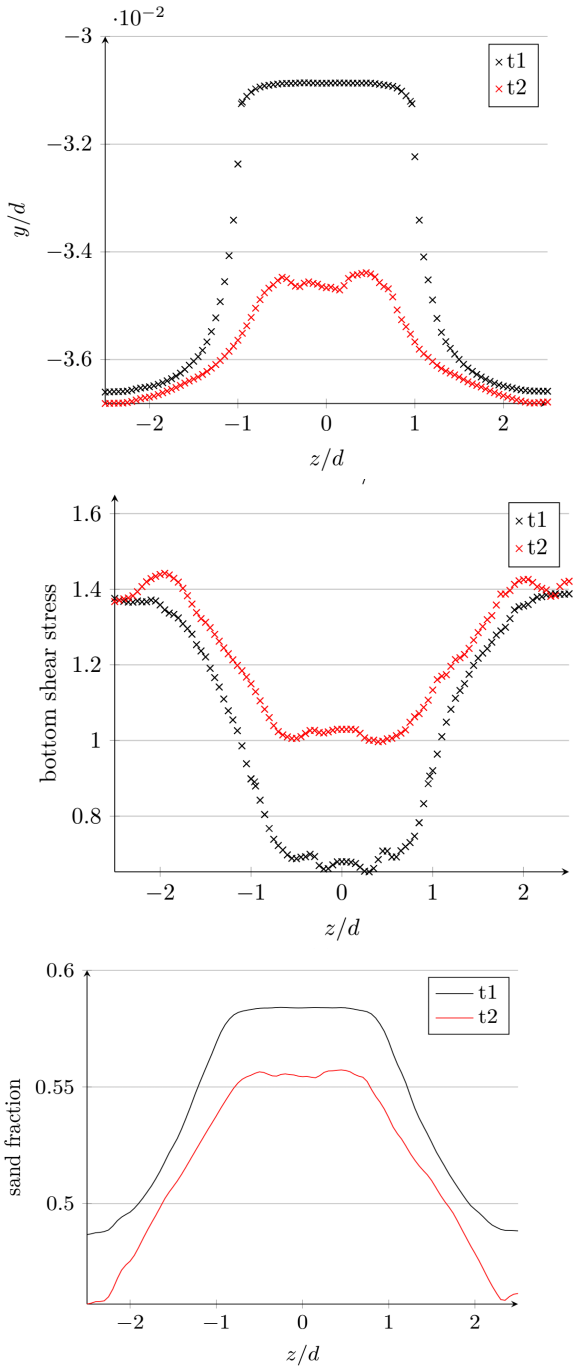

Fig. 9. Temporal evolution between t1 and t2=t1+1s of (a) the bottom elevation (up), (b) bottom shear stress (middle) and (c) the sand fraction (bottom) at x/d=8.125.

The eroded sand is then either deposited at 6.75d (as shown in figure 8(b)), or suspended in the vertical wise, or transported by the wake to occur degraded bed crests following the wake progression in the downstream of the rotor (as shown in figure 6).

Figure 8(c) and figure 9, show a significant transport of sand taken place at x=8.125d mainly close to the two lateral borders. This phenomenon is a result of the fluid acceleration around the turbine and the reduction of the velocity in the turbine's wake (see figure 7).
Figure 9(c) presents the evolution of the sand fraction at x/d=8.125 between t1=17s and t2=t1+1=18s. Everywhere

along the bottom at this x-location, the sand fraction is decreasing, and the shear stress is increasing (Figure 9a). The sediment is easier to erode then. Inversely to the use of a classical two-layer model based on the Exner equation, the critical bottom shear stress is not used here as a threshold to trigger the erosion process. In that case the concentration is reducing then the sediment is easier to be entrained by the flow.

Figure 10 shows the impact of the presence of the turbine on the bed evolution. Below the turbine at x/d=5.25 the presence of turbine leads to an erosion of sediment layer about (0.024-0.03) compared to baseline results, the eroded sand are then deposited at x/d=6.75. There is no erosion due to the turbine in the centre of the canal at the location x/d=8.125.

From this figure, the impact of the turbine rotation on the sediment bed can be identified by considering the symmetry (or not) of the bottom evolution. At the location x/d=5.25, the erosion is higher on the right part. This effect is less evident to see at the location x/d=6.75, Which indicates the limit of the rotation effect. Then the bottom evolution is completely symmetric at x/d=8.125, there is no more effect of the turbine rotation. Moreover, an excess of erosion is identified at this location on both sides of the canal. The rotation of the turbine has no more effect but the reducing of the flow in the wake and the acceleration of the flow around the turbine due to the blockage effects should be responsible to those symmetrical lateral erosions.

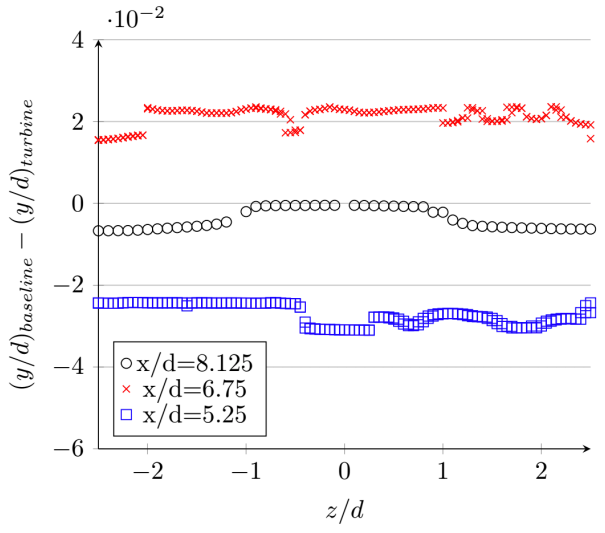

Fig. 10. Difference in dimensionless bed elevation between the baseline results and turbine results at t=17s. The erosion is represented is negative values.

IV. CONCLUSIONS AND PERSPECTIVES

The research program carried out during this work aim to couple the 3D Euler multi-phase model CFD approach to a BEMT model of an axial-flow three-bladed hydrokinetic turbine to study the interactions between the turbine and sediment transport of sandy bed. A validation of the different part of the model has been done. A first study of the erosion of a bottom substrate has been conducted. The energy extracted by the turbine alters the hydrodynamics of the stream by increasing or reducing the friction in areas around the turbines. Close to the turbine, scour phenomena and deposit zones are appearing. In the first seconds a large dynamic of the bottom is observed, then a stabilization of the bottom level is reached. The turbine rotation induces a non-symmetric repartition of the bed evolution, and the blockage effect is responsible to a symmetrical lateral erosion in the turbine's wake.

Those morphology changes should be more important in real rivers and should have an impact on ecological processes. In the near field, the high levels of suspended sediment could affect the surrounding water quality and increase turbidity level by reducing the light penetration in water, the temperature and the aquatic habitat. Moreover, metallic contaminants could be trapped in the sediment bed [14] and be reintroduced in the water column by the erosion of the bed.

Large scales morphological evolution have been also considered such as the dunes' migration [4]. It could modify the turbulent boundary layer and cause time-varying turbulent structures. It could then affect human daily activities such as farming [15] and can lead to economic losses and damages in long term due to land collapse…

The river morphology changes need thorough investigation as any excessive development may also contribute to several impacts. There remains a need for a systematic investigation on turbine-sediment interactions in real scale river application.

REFERENCES

[1] http://www.hydroquest.net/

[2] Sánchez M., Carballo R., Ramos V., Iglesias G., Tidal stream energy impact on the transient and residual flow in an estuary: A 3D analysis. Applied Energy, 116, 167–177, 2014.

[3] Fairley I., Masters I., Karunarathna H., The cumulative impact of tidal stream turbine arrays on sediment transport in the Pentland Firth, Renewable Energy, Volume 80, 755-769, 2015.

[4] Hill C., Musa M., Guala M., Interaction between instream axial flow hydrokinetic turbines and uni-

directional flow bedforms, Renewable Energy, Volume 86, 409-421, 2016.

[5] Chauchat J., and Guillou S., On turbulence closures for two-phase sediment-laden flow models, J. Geophys. Res., 113, C11017, 2018.

[6] Cyrille Bonamy, Julien Chauchat, Zhen Cheng, Tim Nagel, Tian-Jian Hsu. sedFoam, a OpenFOAM solver for sediment transport. *12th OpenFoam Workshop*, Jul 2017, Exeter, United Kingdom.

[7] Cheng Z., Hsu T.-J., Calantoni J. SedFoam: A multi-dimensional Eulerian two-phase model for sediment transport and its application to momentary bed failure. Coastal Engineering, 119, 32-50, 2017.

[8] Malki R., Williams A.J., Croft T.N., Togneri M., Masters I., A coupled blade element momentum – Computational fluid dynamics model for evaluating tidal stream turbine performance, Applied Mathematical Modelling, Volume 37, Issue 5, 3006-3020, 2013.

[9] Shives M., Crawford C., Adapted two-equation turbulence closures for actuator disk RANS simulations of wind & tidal turbine wakes, Renewable Energy, vol. 92(C), 273-292, 2016.

[10] Barbry N., Guillou S. et Nguyen K.D., Une approche diphasique pour le calcul du transport sédimentaire en milieux estuariens, Comptes Rendus de l'Académie des Sciences, Série II.b, 328 (11), 793-799, 2000.

[11] Hsu T-J, Jenkins J., Liu P., On two-phase sediment transport: Sheet flow of massive particles. Proceedings of The Royal Society A: Mathematical, Physical and Engineering Sciences, 460. 2223-2250, 2004.

[12] Pham van bang D., Lefrançois E., Sergent P. Bertrand F., MRI experimental and finite elements modelling of the sedimentation-consolidation of mud, La Houille Blanche, 3, 39-44, 2008.

[13] Mycek P., Gaurier B., Germain G., Pinon G., Rivoalen E., Experimental study of the turbulence intensity effects on marine current turbines behaviour, Part I: One single turbine. Renewable Energy, 66, 729-746, 2014.

[14] Coynel A., Gorse L., Curti C., Schafer J., Grosbois C., Morelli G., Ducassou E., Blanc G., G.M., Mojtahid M., Spatial distribution of trace elements in the surface sediments of a major European estuary (Loire Estuary, France): Source identification and evaluation of anthropogenic contribution, Journal of Sea Research, 118, 77–91, 2016.

[15] Awang Ali, Awang Nasrizal and Ariffin, Junaidah and Razi, Mohd and Abdullah, Jazuri. (2017). Environmental Degradation: A Review on the Potential Impact of River Morphology. MATEC Web of Conferences. 103. 04001. 10.1051/matecconf/201710304001.